Concentration-dependent supramolecular patterns of C_3 and C_2 symmetric molecules at the solid/liquid interface

Mohamed El Garah,[a] Timothy R. Cook,[b] Hajar Sepehrpour,[b] Artur Ciesielski,[a,*] Peter, J. Stang [b,*] and Paolo Samorì [a,*]

[a] University of Strasbourg, CNRS, ISIS UMR 7006, 8 allée Gaspard Monge, F-67000 Strasbourg, France. E-mail: ciesielski@unistra.fr, samori@unistra.fr

[b] Department of Chemistry, University of Utah, 315 South 1400 East, Room 2020, Salt Lake City, Utah 84112, United State. E-mail: stang@chem.utah.edu

Highlights:

- Porous and densely packed monolayer are prepared onto graphite surface.
- Physisorbed monolayers are carried out by mean of scanning tunneling microscopy.
- C3 and C2 molecular symmetries are investigated on graphite surface.
- The understanding of intermolecular and molecule-substrate interaction is provided.

Abstract

Here we report on a scanning tunnelling microscopy (STM) investigation on the self-assembly of C_3- and C_2-symmetric molecules at the solution/graphite interface. 1,3,5-tris((E)-2-(pyridin-4-yl)vinyl)benzene and 1,1,2,2-tetrakis(4-(pyridin-4-yl)phenyl)ethane are used as model systems. These molecules displayed a concentration dependent self-assembly behaviour on graphite, resulting in highly ordered supramolecular structures, which are stabilized jointly by van der Waals substrate-adsorbate interactions and in-plane intermolecular H-bonding. Denser packing is obtained when applying a relatively high concentration solution to the basal plane of the surface whereas a less dense porous network is observed upon lowering the concentration. We show that the molecular conformation does not influence the stability of the self-assembly and a twisted molecule can pack into dense and porous architectures under the concentration effect.

1. Introduction

Molecular self-assembly at surfaces and interfaces has been widely exploited during the last three decades to nanopattern surfaces with an atomic precision, becoming a reliable route to generate functional nanostructures [1, 2]. The virtually unlimited degrees of freedom offered by organic chemistry grant access to molecules possessing different sizes and characterized by multiple and regiospecific substitutions with functional groups at the core, in the scaffold and/or in the periphery [3, 4]. In this framework, π-conjugated molecules exhibit unique opto-electronic properties, which render them interesting building blocks for application in opto-electronics [5, 6].

In general, the self-assembly of molecules at surfaces and interfaces is ruled by the interplay of intramolecular, intermolecular and interfacial forces. The use of a rigid π-conjugated scaffold limits, to a certain extent, the conformational degrees of freedom of the molecules [7]. On the other hand, the functionalization of the molecular peripheries with specific moieties enables the use of dipolar interactions to stabilize in-plane adjacent molecules, resulting in controlled two-dimensional (2D) crystallization and ultimately the formation of robust self-assembled networks [8-10]. Among non-covalent interactions, hydrogen bonding combines specificity, cooperativity, reversibility and directionality, the latter offering high control over the geometry of the assemblies [11-15]. H-bonding occurs between polar molecules where a hydrogen (H) atom can interact with more electronegative atoms such as oxygen (O) or nitrogen (N). It has been exploited to design and to build various molecular nano-architectures, in particular on solid surfaces resulting in linear and cyclic motifs [16-21].

Both the structure of chemisorbed and physisorbed molecular self-assembled monolayers, as well as their nanoscale electronic density states on electrically conductive solid surfaces, can

be explored by means of scanning probe techniques, and in particular by scanning tunnelling microscopy (STM), which has proven to be the most convenient tool to probe the physisorbed molecules with sub-molecular resolution in real space. It is an excellent tool to unravel structure and dynamics of molecules at surfaces under different environmental conditions including ultra-high vacuum (UHV), solid/air or solid/liquid interface. The latter environment offers many advantages when performing molecular self-assembly studies: (i) the experiments do not require a complicated or expensive set-up, (ii) it facilitates choice of the solvent in view of the selected solute and substrate, (iii) it allows the investigation of large molecules that can be difficult to sublime under vacuum, (iv) the reversible nature of self-assembly enables defect reparation *via* self-healing by taking advantage of the dynamic exchange between the liquid phase and the adsorbed molecules [8, 22]. Working at the solid/liquid interface environment, the nanostructures can be influenced by a number of experimental conditions such as the chosen solvents, [23-26] the temperature, [27-29] and the concentration [30-33]. The formation of concentration-dependent nanostructures at surfaces and interfaces is a 2D crystallization phenomenon. It has been shown that densely packed molecular assemblies are produced when operating at a relatively high concentration and the porous networks are obtained at low concentration [34-36]. It is however important to note that the range of concentrations in which one phase is favoured over the other cannot be generalized. The strength of both inter and intramolecular forces varies from one molecule to the others and it is moderated also by the chosen solvent. Controlling the formation of the concentration-dependent 2D molecular networks can therefore be considered as a key factor to tune the self-assembly on surfaces [37, 38].

The concentration-dependent self-assembly of C_3-symmetric molecules has been reported in the literature but to the best of our knowledge C_2-symmetric molecules are not yet investigated for concentration effects. The molecular symmetry C_3 refers to obtaining the

equivalent configurations by a rotation of the molecule around an axis with 120° while the symmetry C_2 takes the molecule to the same structure by a rotation of 180°.

In this work, we report on the STM investigation of a concentration dependent formation of 2D molecular self-assembly at the solid/liquid interface. We focus our attention on two molecular building blocks with C_3 and C_2-symmetry. 1,3,5-tris((E)-2-(pyridin-4-yl)vinyl)benzene (**3Py**) and 1,1,2,2-tetrakis(4-(pyridin-4-yl)phenyl)ethane (**4Py**) are physisorbed on highly oriented pyrolitic graphite (HOPG) surface. In both molecules the pyridyl N atom in the *para* position promotes the formation of directional H-bonds [34, 35]. The choice of pyridine based chemistry enables the formation of weak hydrogen bonding, resulting in the generation of directional H-bonds that operate under full thermodynamic control [34-36, 39, 40].
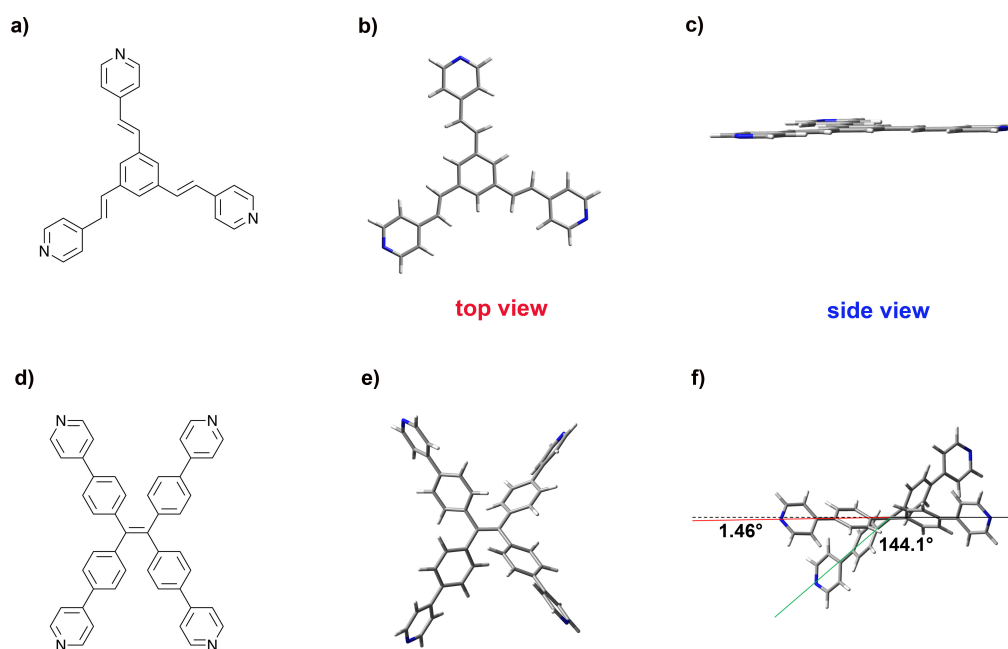
2. Results and Discussion

Fig. 1. Chemical structure (a), top (b) and side view (c) of optimized geometry of 1,3,5-tris((E)-2-(pyridin-4-yl)vinyl)benzene (**3Py**). Chemical structure (d), top (e) and side view (f) of optimized geometry of 1,1,2,2-tetrakis(4-(pyridin-4-yl)phenyl)ethane (**4Py**).

Figure 1 displays the chemical structure and the optimized geometries of the C_3-symmetric **3Py** and the C_2-symmetric **4Py**. The geometry optimization was done in the gas phase using density functional theory (DFT) calculations with three-parameter hybrid exchange functional combined with the Lee–Yang–Parr correlation functional (B3LYP) and 6-31G basis set within Gaussian 09 [41]. **3Py** exhibits a flat stilbene core with a *trans* configuration, whereas **4Py** exhibits a twisted configuration due the steric hindrance brought into play by the interaction among the protons decorating the closest phenyl rings.

As previously reported, [34, 35, 39] triangular molecules can assemble on solid surfaces in parallel (P) or anti-parallel (A) fashion. Two different self-assembly motifs formed through (pyridyl)N⋯H−C(pyridyl) H-bonds can be proposed for **3Py**, and are characterized by the formation of P1 and P2 pairing (see the Figure 2a,). Such pairing allows the generation of three distinct self-assembly motifs, i.e. $[\textbf{3Py}]_n P1$, $[\textbf{3Py}]_n A1$ and $[\textbf{3Py}]_n P2$ (Figure 2a). $[\textbf{3Py}]_n P1$ and $[\textbf{3Py}]_n A1$ display dense parallel and anti-parallel molecular packing respectively while $[\textbf{3Py}]_n P2$ features a parallel porous network. On the other hand, since **4Py** has a C_2 symmetry, it can be self-assembled only in the parallel configurations P1 and P2 *via* H-bonds (Figure 2b). Such interactions can promote the molecular packing of **4Py** into two supramolecular architectures, i.e. the dense $[\textbf{4Py}]_n P1$ and the porous $[\textbf{4Py}]_n P2$ motif (Figure 2b).
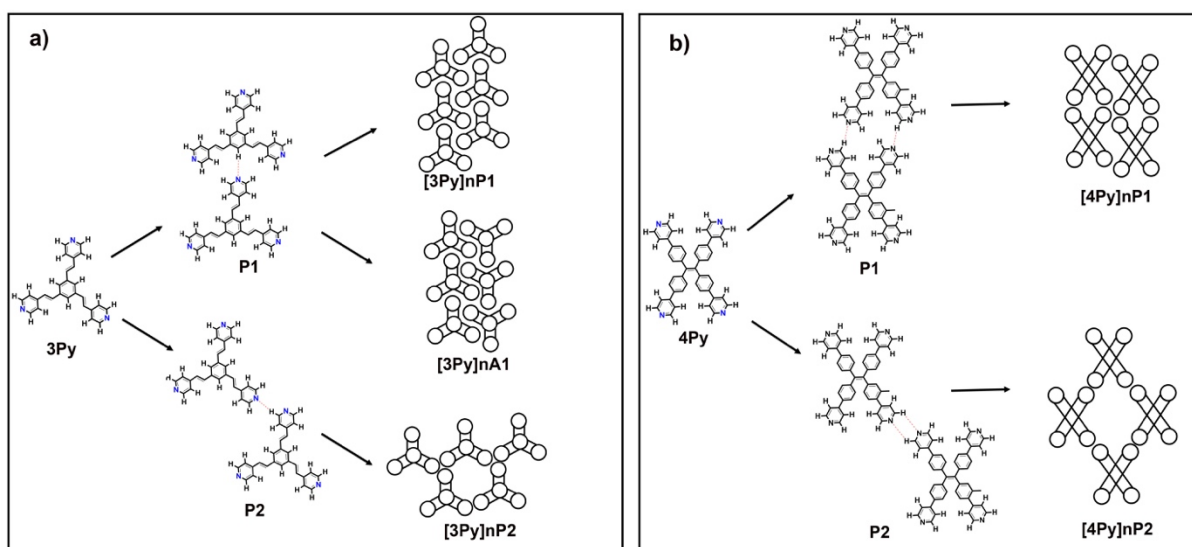
Fig. 2. a) Three possible configurations of C_3-symmetric **3Py**. b) Two possible configurations of C_2-symmetric **4Py** molecule. The intermolecular interactions are based on (pyridyl)N$\cdots$H−C(pyridyl) H-bond connections. (P) for parallel and (A) for anti-parallel fashion.

The molecular self-assembly at the solid/liquid interface on HOPG was explored *in-situ* by STM. A 4 μL droplet of a 250 μM solution of **3Py** in 1-phenyloctane was drop cast on a freshly cleaved surface. Figure 3a displays a STM height image of the physisorbed monolayer. It shows a 2D densely packed network of molecules lying flat on the basal plane of the surface. Due to their extended π-conjugated system, the individual molecules in the self-assembled pattern appear bright and exhibit a C_3-symmetric contrast. All the molecules are oriented along the same direction with a parallel configuration. **3Py** is adsorbed in parallel fashion leading then to dense molecular architectures that are stable for 3-4 hours. The 2D self-assembly can be described by the formation of six (pyridyl)N$\cdots$H−C(pyridyl) H-bonds per molecule. A representative molecular model is presented in Figure 3b.
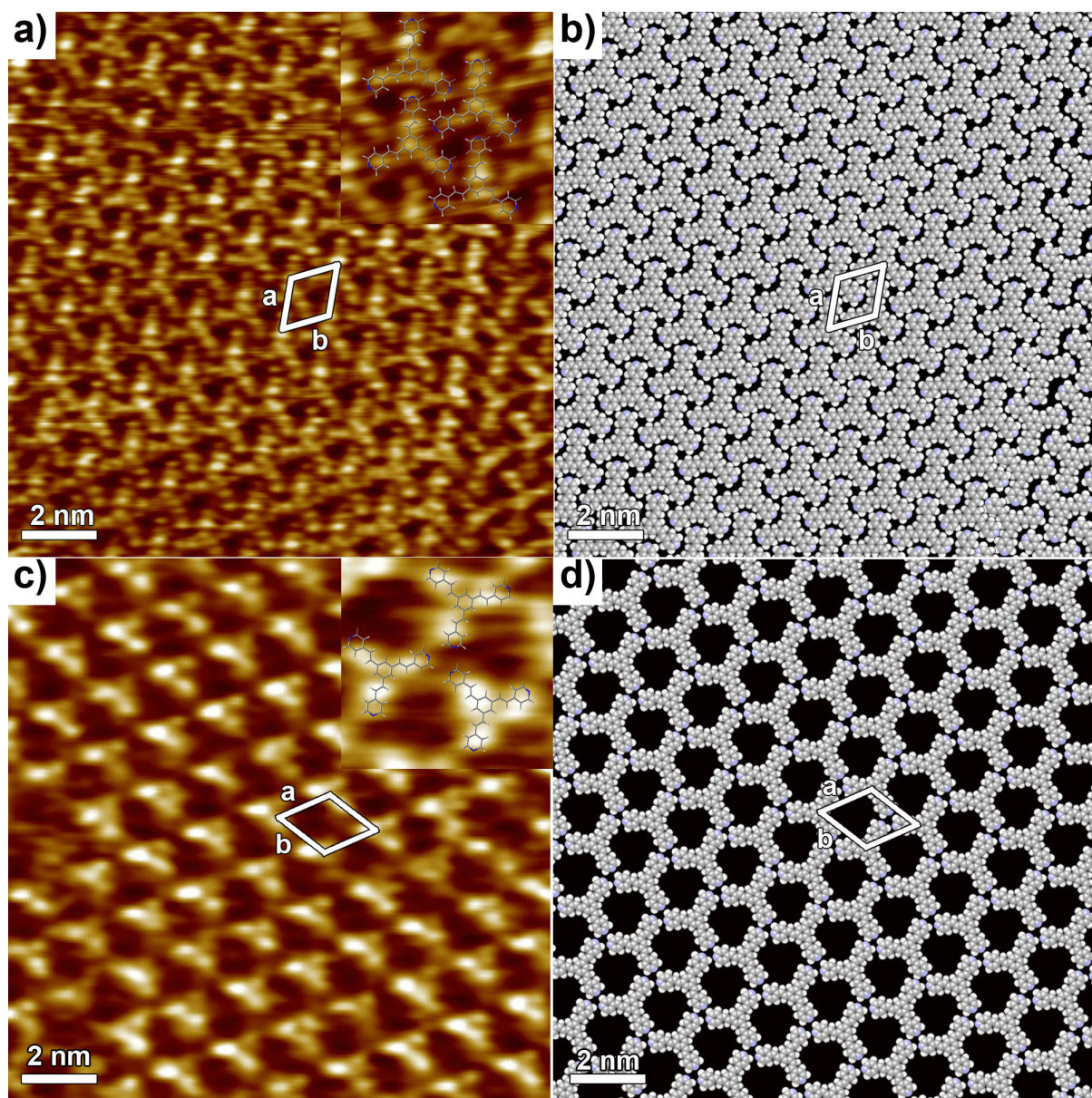
Fig. 3. STM height images and proposed packing motifs of **3Py** at the solid/liquid interface. Solutions applied to the surface: (a-b) *concentration* = 200 −300 μM, and (c-d) *concentration* = 50 −150 μM. Tunnelling parameters: (a) average tunnelling current (I_t) = 25 pA, tip bias (V_t) = 400 mV; (c) I_t = 25 pA, V_t = 600 mV. Insets: (a, c) 3.6×3.6 nm^2.

We then extended our investigation to the formation of **3Py** films by lowering the concentration of the solution applied to the surface. STM height image in Figure 3b displays the physisorbed monolayer of **3Py** at the solid/liquid interface obtained with a concentration of 100 μM. The polycrystalline structure consists of a 2D porous architecture. Each single

3Py molecule appears as three bright protrusions that are related to the electronic density of its conjugated phenyls. Similarly, to the previous packing, **3Py** lies flat on the surface leading to the formation of a porous network at low concentration. The molecular packing can be described by the formation of six (pyridyl)N⋯H−C(pyridyl) H-bonds per molecule, as evident in the model displayed in Figure 3d. The formation of such molecular packing is consistent with the predicted [**3Py**]$_n$P2 structure as illustrated in the Figure 2a. Interestingly, a concentration-dependent self-assembly study of **3Py** reveals the formation of two supramolecular structures with parallel rearrangement highlighting the strength of the intermolecular interactions. Dense [**3Py**]$_n$P1 and porous [**3Py**]$_n$P2 networks have been seen at 1-phenyloctane/HOPG interface. On the basis of the previous work, [34] one can likely conclude that the anti-parallel [**3Py**]$_n$A1 self-assembly is energetically unfavourable.

For all crystalline 2D patterns the unit cell parameters, that is, the length of the vectors a and b, the angle between the vectors (α), the unit cell area (A), the number of molecules in the unit cell (N_{mol}) and the area occupied by a single molecule in the unit cell (A_{mol}, with $A_{mol} = A/N_{mol}$) are given in Table 1.

Table 1. Unit cell parameters of the structure [**3Py**]$_n$P1, [**3Py**]$_n$P2, [**4Py**]$_n$P1 and [**4Py**]$_n$P2,

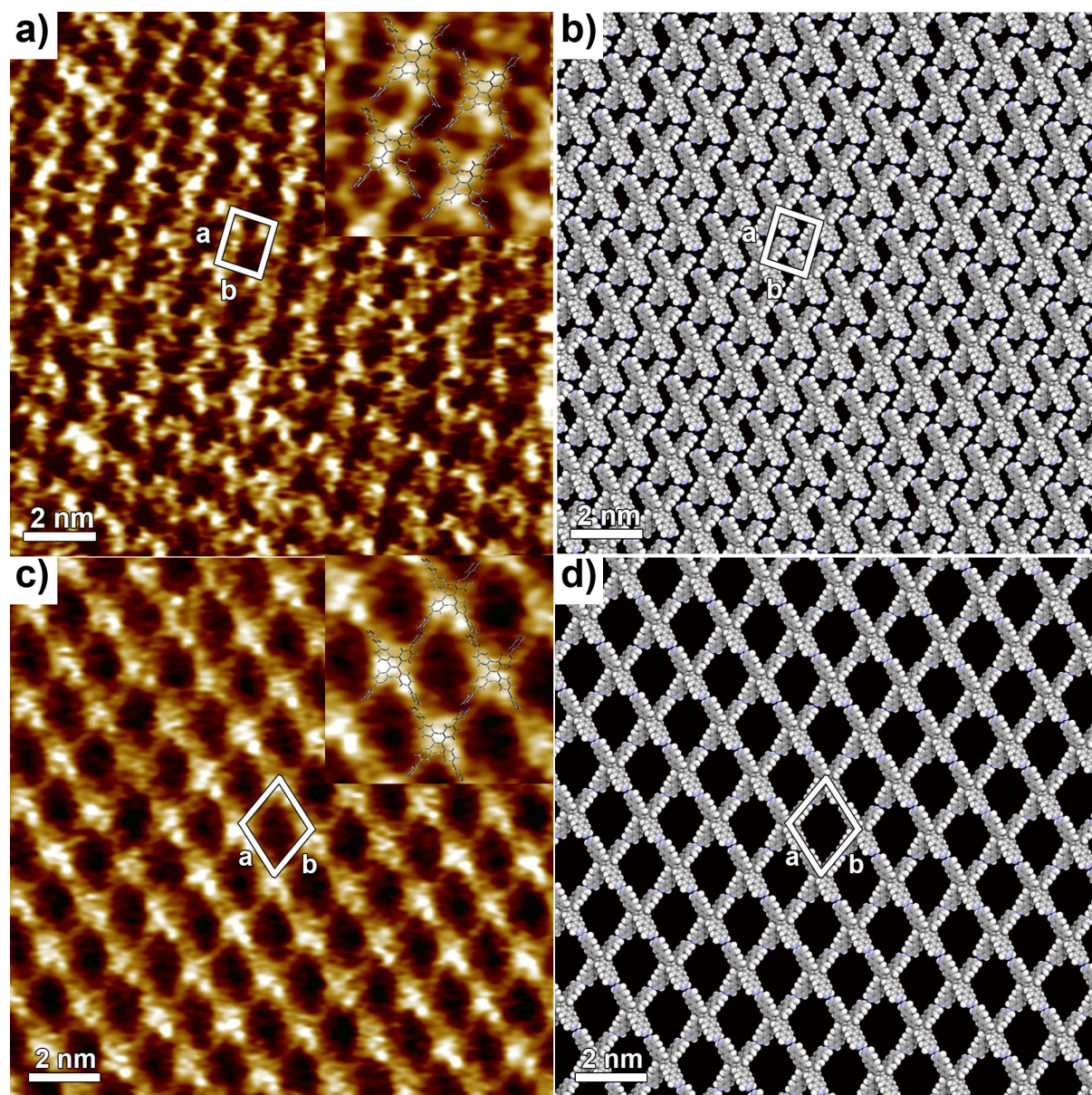| Structure	a [nm]	b [nm]	α [°]	A [nm^2]	N_{mol}	A_{mol} [nm^2]
[**3Py**]$_n$P1	1.4 ± 0.1	1.4 ± 0.1	60 ± 2	1.7 ± 0.1	1	1.7 ± 0.1
[**3Py**]$_n$P2	1.6 ± 0.1	1.6 ± 0.1	60 ± 2	2.2 ± 0.1	1	2.2 ± 0.1
[**4Py**]$_n$P1	1.6 ± 0.1	1.3 ± 0.1	90 ± 2	2.1 ± 0.1	1	2.1 ± 0.1
[**4Py**]$_n$P2	1.7 ± 0.1	1.7 ± 0.1	60 ± 2	2.5 ± 0.1	1	2.5 ± 0.1

Fig. 4. STM height images and proposed packing motifs of **4Py** at the solid/liquid interface. Solutions applied to the surface: (a-b) *concentration* = 60 − 150 μM, and (c-d) *concentration* = 20 − 60 μM. Tunnelling parameters: (a) I_t = 25 pA, V_t = 650 mV; (c) I_t = 25 pA, V_t = 450 mV. Insets: (a, c) 4.6×4.6 nm^2.

We then focused our attention on the study of the self-assembly of the C_2-symmetric **4Py** at the solid/HOPG interface. This molecule, which exhibits four pyridines units with an N atom in the *para* position, adopts a twisted conformation in the gas phase yielding a cross-like

shape. We prepared **4Py** solutions in CHCl$_3$ and further diluted it in 1-phenyloctane to reach concentrations ranging from 10 to 150 µM. A 4 µL of a 100 µM solution of **4Py** was applied onto a freshly cleaved HOPG surface. Figure 4a displays STM image of the **4Py** physisorbed monolayer. The film exhibits of 2D densely packed network consisting of linear bright arrays that are stable for 3-4 hours. The molecular model is displayed in Figure 4b. The self-assembly can be explained by the formation of eight (pyridyl)N···H−C(pyridyl) H-bonds per molecule according to the [**4Py**]$_n$P1 structure (see Figure 2b). Moreover, upon increasing the concentration of the **4Py** solution applied to the HOPG surface up to 150 µM, the same densely packed network was monitored by STM.

Conversely, when the solution concentration cast to the HOPG surface is lowered to 50 µM, a more loosely packed porous diamond-like supramolecular motif is observed (Figure 4c), which is stable for 3-4 hours. The unit cell parameters are given by a = b = 1.7 ± 0.1 nm, α = 60º ± 2º, leading to an area of A = 2.5 ± 0.1 nm^2 where each unit cell contains a single molecule. Each single bright protrusion appears symmetric and contains four edges (Figure 4c). Two diagonal edges are thicker (vector a) than the others (vector b). The symmetric single bright protrusion matches well with the structure of the **4Py** molecule. The contrast difference of the edges (Figure 4c) can be ascribed to the twisted conformation of adsorbed **4Py** on the surface. Compared to the previous architecture obtained at higher concentration, the one displayed in Figure 4c exhibits a porous packing. This molecular self-assembly resulted from the formation of eight (pyridyl)N···H−C(pyridyl) H-bonds per molecule, i.e two H-bonds by the pyridine group (edge). Figure 4d displays the molecular model of the porous **4Py** structure which is consistent with the [**4Py**]$_n$P2 predicted structure (see Figure 2b). Through these experiments, we thermodynamically controlled the formation of dense and porous networks using a C_2-symmetric molecular building block at the solid/liquid

interface. We highlighted the role of H-bonds on the stabilization of the molecular architectures under the concentration effect.

Few results have been reported thus far on the thermodynamic control of supramolecularly organized thin films formed under concentration effect at the solid/liquid interface. Both mono-[33, 36, 42] and multicomponents structures have been investigated [43]. We limit our discussion to the study of monocomponent C_3-symmetric molecules, especially those containing the pyridine units. STM and Monte Carlo simulations have been carried out to predict the self-assembly of 1,3,5-tris(pyridine-4-ylethynyl)benzene (**1**) onto the HOPG surface [34]. Dense and porous architectures were formed based on H-bonds at high and low concentrated solution, respectively.[34] De Feyter and co-workers have recently reported on the study of 4,4',4''-((2,4,6-trimethylbenzene-1,3,5-triyl)tris(ethyne-2,1-diyl))tripyridine (**2**), a similar molecule to **1** but with three CH_3 groups on the central phenyl ring [39]. A Close-packed network was formed at high concentration and two less dense structures were observed at low concentration. By comparing the two molecules, **2** results in the formation of anti-parallel structures [39] where **1** [34] is based on the parallel arrangement. No porous network of **2** was observed at low concentration. The composition of the self-assembly of **1** and **2** therefore reveals that the subtle addition of methyl groups yields a major changed in the self-assembly at surfaces and molecular rearrangement under the concentration effect. On the other hand, we recently showed the effect of the position of N atom in the pyridine unit by studying the 1,3,5-tris(pyridine-4-ylethynyl)benzene with the N in the *meta* position (**3**). In the latter molecule, fourteen supramolecular motifs have been predicted theoretically using DFT calculations depending on the molecular density on the surface [35]. In contrast, STM experiments have revealed the formation of only four favourable supramolecular structures ranging from the dense to the porous networks by lowering the concentration of the solution

cast at surfaces [35]. All the resulting molecular architectures are stabilized by the formation of H-bonds.

By comparing the molecule **3Py** here investigated to **1**, a similar behaviour was seen by adopting the parallel molecular rearrangement [34]. The dense self-assembly was obtained at high concentration while the porous network resulted at low concentration. In contrast to C_3-symmetric molecules previously discussed, **4Py** featuring a C_2 symmetry also reveals a rich concentration-dependent self-assembly behaviour at the solid/liquid interface. Stabilized by H-bonds, dense and porous networks were obtained at high and law concentration, respectively. Despite the twisted conformation adopted by **4Py**, the H-bonds were sufficiently strong to thermodynamically stabilize the dense and the porous structures. This kind of 2D molecular crystallization reveals that the concentration-dependent strategy is not affected by the molecular symmetry, even if the symmetry can be considered as a powerful remote control to tune the size of the nanopores. Controlling the size and the shape of these nanocavities may be interesting to optimize the selectivity of guest molecules, e.g. for application in sensing.

3. Conclusion

We have reported on the concentration-dependent formation of the molecular self-assemblies of C_3- and C_2-symmetric molecules at the solid/liquid interface. We have demonstrated the formation of dense and porous networks at high and low concentration, respectively. C_3-symmetric molecule, with a flat core, led to the formation of dense and porous architectures based on parallel molecular arrangement on the surface. We have also showed that the C_2-symmetric molecule packed into dense and porous networks under the concentration effect. Morphologically, its twisted conformation was found not to hinder the molecular self-

assembly into spatially extended and stable 2D networks. All structures are stabilized by weak intermolecular H-bonds between the pyridine moieties, resulting in full thermodynamic control. Forming molecular architectures with uniform porosity at low concentration could be attractive for the encapsulation of guest molecules, thus for application in sensing. The development of molecular design strategies on solid surfaces will also offer the opportunity to tune the function of organic ultrathin films.

4. Experimental section

STM measurements were performed using a Veeco scanning tunneling microscope (multimode Nanoscope III, Veeco) at the interface between a highly oriented pyrolitic graphite (HOPG) substrate and a supernatant solution, thereby mapping a maximum area of 1×1 μm. The solution of the molecule was applied to the basal plane of the surface. For STM measurements, the substrates were glued to a magnetic disk and an electric contact was made with silver paint (Aldrich Chemicals). The STM tips were mechanically cut from a Pt/Ir wire (90/10, diameter 0.25 mm). The raw STM data were processed through the application of background flattening and the drift was corrected using the underlying graphite lattice as a reference. The lattice was visualized by lowering the bias voltage to 20 mV and raising the

current up to 65 pA. Solutions were made by dissolving **3Py** and **4Py** in chloroform followed by a dilution in 1-phenyloctane. STM imaging was carried out in constant current mode. Monolayer pattern formation was achieved by applying 4 µL of solution onto freshly cleaved HOPG. The STM images were recorded at room temperature once a negligible thermal drift was achieved. The molecular models were minimized with DFT and processed with QuteMol visualization software (http://qutemol.sourceforge.net).

References

[1]   J.V. Barth, G. Costantini, K. Kern, Engineering atomic and molecular nanostructures at surfaces, Nature, 437 (2005) 671-679.
[2]   J.C. Love, L.A. Estroff, J.K. Kriebel, R.G. Nuzzo, G.M. Whitesides, Self-Assembled Monolayers of Thiolates on Metals as a Form of Nanotechnology, Chem. Rev., 105 (2005) 1103-1170.
[3]   J.-M. Lehn, Perspectives in Supramolecular Chemistry—From Molecular Recognition towards Molecular Information Processing and Self-Organization, Angew. Chem. Int. Ed., 29 (1990) 1304-1319.
[4]   T. Weil, T. Vosch, J. Hofkens, K. Peneva, K. Müllen, The rylene colorant family—tailored nanoemitters for photonics research and applications, Angew. Chem. Int. Ed., 49 (2010) 9068-9093.
[5]   Y. Shirota, Organic materials for electronic and optoelectronic devices, J. Mater. Chem., 10 (2000) 1-25.
[6]   A.P.H.J. Schenning, E.W. Meijer, Supramolecular electronics; nanowires from self-assembled [small pi]-conjugated systems, Chem. Commun., (2005) 3245-3258.
[7]   C.-A. Palma, P. Samorì, M. Cecchini, Atomistic Simulations of 2D Bicomponent Self-Assembly: From Molecular Recognition to Self-Healing, J. Am. Chem. Soc., 132 (2010) 17880-17885.
[8]   A. Ciesielski, C.-A. Palma, M. Bonini, P. Samorì, Towards Supramolecular Engineering of Functional Nanomaterials: Pre-Programming Multi-Component 2D Self-Assembly at Solid-Liquid Interfaces, Adv. Mater., 22 (2010) 3506-3520.
[9]   D. Bonifazi, S. Mohnani, A. Llanes-Pallas, Supramolecular Chemistry at Interfaces: Molecular Recognition on Nanopatterned Porous Surfaces, Chem. Eur. J., 15 (2009) 7004-7025.
[10]   J.V. Barth, Molecular Architectonic on Metal Surfaces, Annu. Rev. Phys. Chem., 58 (2007) 375-407.
[11]   R.P. Sijbesma, E.W. Meijer, Self-assembly of well-defined structures by hydrogen bonding, Curr. Opin. Colloid Interface Sci., 4 (1999) 24-32.
[12]   D.C. Sherrington, K.A. Taskinen, Self-assembly in synthetic macromolecular systems multiple hydrogen bonding interactions, Chemi. Soc. Rev., 30 (2001) 83-93.
[13]   S. Vijayaraghavan, D. Ecija, W. Auwärter, S. Joshi, K. Seufert, M. Drach, D. Nieckarz, P. Szabelski, C. Aurisicchio, D. Bonifazi, J.V. Barth, Supramolecular

Assembly of Interfacial Nanoporous Networks with Simultaneous Expression of Metal–Organic and Organic-Bonding Motifs, Chem. Eur. J., 19 (2013) 14143-14150.

[14] D. Ecija, S. Vijayaraghavan, W. Auwärter, S. Joshi, K. Seufert, C. Aurisicchio, D. Bonifazi, J.V. Barth, Two-Dimensional Short-Range Disordered Crystalline Networks from Flexible Molecular Modules, ACS Nano, 6 (2012) 4258-4265.

[15] T. Kaposi, S. Joshi, T. Hoh, A. Wiengarten, K. Seufert, M. Paszkiewicz, F. Klappenberger, D. Ecija, L. Đorđević, T. Marangoni, D. Bonifazi, J.V. Barth, W. Auwärter, Supramolecular Spangling, Crocheting, and Knitting of Functionalized Pyrene Molecules on a Silver Surface, ACS Nano, 10 (2016) 7665-7674.

[16] K.G. Nath, O. Ivasenko, J.A. Miwa, H. Dang, J.D. Wuest, A. Nanci, D.F. Perepichka, F. Rosei, Rational modulation of the periodicity in linear hydrogen-bonded assemblies of trimesic acid on surfaces, J. Am. Chem. Soc., 128 (2006) 4212-4213.

[17] X. Zhang, Q. Zeng, C. Wang, Molecular templates and nano-reactors: two-dimensional hydrogen bonded supramolecular networks on solid/liquid interfaces, RSC Adv., 3 (2013) 11351-11366.

[18] M. Lackinger, W.M. Heckl, Carboxylic Acids: Versatile Building Blocks and Mediators for Two-Dimensional Supramolecular Self-Assembly, Langmuir, 25 (2009) 11307-11321.

[19] D.L. Keeling, N.S. Oxtoby, C. Wilson, M.J. Humphry, N.R. Champness, P.H. Beton, Assembly and Processing of Hydrogen Bond Induced Supramolecular Nanostructures, Nano Lett., 3 (2003) 9-12.

[20] S. De Feyter, A. Miura, S. Yao, Z. Chen, F. Würthner, P. Jonkheijm, A.P.H.J. Schenning, E.W. Meijer, F.C. De Schryver, Two-dimensional self-assembly into multicomponent hydrogen-bonded nanostructures, Nano Lett., 5 (2005) 77-81.

[21] A. Ciesielski, S. Lena, S. Masiero, G.P. Spada, P. Samorì, Dynamers at the Solid–Liquid Interface: Controlling the Reversible Assembly/Reassembly Process between Two Highly Ordered Supramolecular Guanine Motifs, Angew. Chem. Int. Ed., 49 (2010) 1963-1966.

[22] S. De Feyter, F.C. De Schryver, Self-Assembly at the Liquid/Solid Interface: STM Reveals, J. Phys. Chem. B, 109 (2005) 4290-4302.

[23] X. Miao, L. Xu, Z. Li, W. Deng, Solvent-induced structural transitions of a 1, 3, 5-tris (10-ethoxycarbonyldecyloxy) benzene assembly revealed by scanning tunneling microscopy, J. Phys. Chem. C, 115 (2011) 3358-3367.

[24] L. Kampschulte, M. Lackinger, A.-K. Maier, R.S. Kishore, S. Griessl, M. Schmittel, W.M. Heckl, Solvent induced polymorphism in supramolecular 1, 3, 5-benzenetribenzoic acid monolayers, J. Phys. Chem. B, 110 (2006) 10829-10836.

[25] Y. Yang, C. Wang, Solvent effects on two-dimensional molecular self-assemblies investigated by using scanning tunneling microscopy, Curr. Opin. Colloid Interface Sci., 14 (2009) 135-147.

[26] Y. Li, Z. Ma, G. Qi, Y. Yang, Q. Zeng, X. Fan, C. Wang, W. Huang, Solvent effects on supramolecular networks formed by racemic star-shaped oligofluorene studied by scanning tunneling microscopy, J. Phys. Chem. C, 112 (2008) 8649-8653.

[27] M.O. Blunt, J. Adisoejoso, K. Tahara, K. Katayama, M. Van der Auweraer, Y. Tobe, S. De Feyter, Temperature-induced structural phase transitions in a two-dimensional self-assembled network, J. Am. Chem. Soc., 135 (2013) 12068-12075.

[28] R. Gutzler, T. Sirtl, J.F. Dienstmaier, K. Mahata, W.M. Heckl, M. Schmittel, M. Lackinger, Reversible phase transitions in self-assembled monolayers at the liquid−solid interface: temperature-controlled opening and closing of nanopores, J. Am. Chem. Soc., 132 (2010) 5084-5090.

[29] C. Marie, F. Silly, L. Tortech, K. Mullen, D. Fichou, Tuning the packing density of 2D supramolecular self-assemblies at the solid− liquid interface using variable temperature, ACS Nano, 4 (2010) 1288-1292.

[30] S. Lei, K. Tahara, F.C. De Schryver, M. Van der Auweraer, Y. Tobe, S. De Feyter, One Building Block, Two Different Supramolecular Surface Confined Patterns: Concentration in Control at the Solid–Liquid Interface, Angew. Chem., Int. Ed., 120 (2008) 3006-3010.

[31] X. Shen, X. Wei, P. Tan, Y. Yu, B. Yang, Z. Gong, H. Zhang, H. Lin, Y. Li, Q. Li, Concentration Controlled Reversible Phase Transitions in Self Assembled Monolayers on HOPG Surfaces, Small, 11 (2015) 2284-2290.

[32] V. Stepanenko, R. Kandanelli, S. Uemura, F. Würthner, G. Fernández, Concentration-dependent rhombitrihexagonal tiling patterns at the liquid/solid interface, Chem. Sci., 6 (2015) 5853-5858.

[33] B. Zha, X. Miao, P. Liu, Y. Wu, W. Deng, Concentration dependent halogen-bond density in the 2D self-assembly of a thiophenanthrene derivative at the aliphatic acid/graphite interface, Chem. Commun., 50 (2014) 9003-9006.

[34] A. Ciesielski, P.J. Szabelski, W. Rżysko, A. Cadeddu, T.R. Cook, P.J. Stang, P. Samorì, Concentration-Dependent Supramolecular Engineering of Hydrogen-Bonded Nanostructures at Surfaces: Predicting Self-Assembly in 2D, J. Am. Chem. Soc., 135 (2013) 6942-6950.

[35] M. El Garah, A. Dianat, A. Cadeddu, R. Gutierrez, M. Cecchini, T.R. Cook, A. Ciesielski, P.J. Stang, G. Cuniberti, P. Samorì, Atomically Precise Prediction of 2D Self-Assembly of Weakly Bonded Nanostructures: STM Insight into Concentration-Dependent Architectures, Small, 12 (2016) 343-350.

[36] S. Lei, K. Tahara, F.C. De Schryver, M. Van der Auweraer, Y. Tobe, S. De Feyter, One Building Block, Two Different Supramolecular Surface-Confined Patterns: Concentration in Control at the Solid–Liquid Interface, Angew. Chem. Int. Ed., 120 (2008) 3006-3010.

[37] U. Mazur, K.W. Hipps, Kinetic and thermodynamic processes of organic species at the solution-solid interface: the view through an STM, Chem. Commun., 51 (2015) 4737-4749.

[38] R. Gutzler, L. Cardenas, F. Rosei, Kinetics and thermodynamics in surface-confined molecular self-assembly, Chem. Sci., 2 (2011) 2290-2300.

[39] A. Mukherjee, J. Teyssandier, G. Hennrich, S. De Feyter, K.S. Mali, Two-dimensional crystal engineering using halogen and hydrogen bonds: towards structural landscapes, Chem. Sci., 8 (2017) 3759-3769.

[40] D. Trawny, P. Schlexer, K. Steenbergen, J.P. Rabe, B. Paulus, H.-U. Reissig, Dense or Porous Packing? Two-Dimensional Self-Assembly of Star-Shaped Mono-, Bi-, and Terpyridine Derivatives, ChemPhysChem, 16 (2015) 949-953.

[41] G.W.T. M. J. Frisch, H. B. Schlegel, G. E. Scuseria, M. A. Robb, J. R. Cheeseman, G. Scalmani, V. Barone, B. Mennucci, G. A. Petersson, H. Nakatsuji, M. Caricato, X. Li, H. P. Hratchian, A. F. Izmaylov, J. Bloino, G. Zheng, J. L. Sonnenberg, M. Hada, M. Ehara, K. Toyota, R. Fukuda, J. Hasegawa, M. Ishida, T. Nakajima, Y. Honda, O. Kitao, H. Nakai, T. Vreven, J. A. Montgomery Jr, J. E. Peralta, F. Ogliaro, M. Bearpark, J. J. Heyd, E. Brothers, K. N. Kudin, V. N. Staroverov, R. Kobayashi, J. Normand, K. Raghavachari, A. Rendell, J. C. Burant, S. S. Iyengar, J. Tomasi, M. Cossi, N. Rega, J. M. Millam, M. Klene, J. E. Knox, J. B. Cross, V. Bakken, C. Adamo, J. Jaramillo, R. Gomperts, R. E. Stratmann, O. Yazyev, A. J. Austin, R. Cammi, C. Pomelli, J. W. Ochterski, R. L. Martin, K. Morokuma, V. G. Zakrzewski, G. A. Voth, P. Salvador, J. J. Dannenberg, S. Dapprich, A. D. Daniels, Ö. Farkas, J.

B. Foresman, J. V. Ortiz, J. Cioslowski and D. J. Fox, Gaussian 09, Gaussian, Inc., Wallingford CT, 2009.

[42]   A. Bellec, C. Arrigoni, G. Schull, L. Douillard, C. Fiorini-Debuisschert, F. Mathevet, D. Kreher, A.-. Attias, F. Charra, Solution-growth kinetics and thermodynamics of nanoporous self-assembled molecular monolayers, J. Chem. Phys., 134 (2011) 124702.

[43]   L. Kampschulte, T.L. Werblowsky, R.S. Kishore, M. Schmittel, W.M. Heckl, M. Lackinger, Thermodynamical equilibrium of binary supramolecular networks at the liquid− solid interface, J. Am. Chem. Soc., 130 (2008) 8502-8507.